

The π Complexation of Alkali and Alkaline Earth Ions by the Use of *meso*-Octaalkylporphyrinogen and Aromatic Hydrocarbons

Lucia Bonomo, Euro Solari, Rosario Scopelliti, and Carlo Floriani*^[a]

Abstract: The full metallation of *meso*-octaalkylporphyrinogens $[\text{R}_8\text{N}_4\text{H}_4]$ (R = Et, **1**; *n*Bu, **2**; CH₂Ph, **3**; (CH₂)₄, **4**) with heavy alkali metals (M = K, Rb, Cs) leads to the porphyrinogen-M₄ compounds, in which the solvation of the alkali cations is largely assured by the intra- and intermolecular π -interactions with the pyrrolyl anions. Such a mode of complexation results in a structural diversity as a function of the *meso* substituents, the size of the metal ion, and the solvent. The structure of the unsolvated polymers $[\text{R}_8\text{N}_4\text{M}_4]_n$ (R = Et, M = K, **5**; M = Rb, **6**; M = Cs, **7**; R = (CH₂)₄, M = Rb, **8**; M = Cs, **9**) have been clarified through the X-ray analysis of **7** recrystallized from diglyme. The structure shows that the tetraanion binds two Cs ions inside the cavity, which display in one case $\eta^1:\eta^1:\eta^1:\eta^1$ and in the other $\eta^5:\eta^5:\eta^5:\eta^5$ interaction modes. Bidimen-

sional polymerization is assured by four Cs ions, which each bind at the η^5 position on the exo face of each pyrrole. With bulkier *meso* substituents, different polymeric forms are obtained (R = *n*Bu, M = K, **10**; M = Rb, **11**; M = Cs, **12**), and their structures were clarified through the X-ray analysis of **10**, which was recrystallized from dimethoxyethane. The polymeric units are made up by the monomeric units $[\text{Bu}_8\text{N}_4\text{K}_2]^{2-}$, in which one potassium is $\eta^1:\eta^1:\eta^1:\eta^5$ and the other $\eta^5:\eta^1:\eta^5:\eta^1$ bonded inside the porphyrinogen cavity. In the case of R = CH₂Ph, the monomeric anion $[(\text{PhCH}_2)_8\text{N}_4\text{K}_2]^{2-}$ (**13**) has been structurally identified. The metallation of **1**

and **2** with active forms of alkaline earth metals (M' = Ca, Sr, Ba) led to dinuclear compounds $[\text{R}_8\text{N}_4\text{M}'_2]$ (R = Et, M' = Ca, **14**; M' = Sr, **15**; M' = Ba, **16**; R = *n*Bu, M' = Ba, **18**), in which both metals inside the cavity are $\eta^1:\eta^3:\eta^1:\eta^3$ (Ca) and $\eta^1:\eta^5:\eta^1:\eta^5$ (Sr and Ba) bonded to the porphyrinogen tetraanion. The coordination sphere of each metal ion is completed by two THF molecules, which, in the case of Ba, are easily replaced by an arene ring $[\text{Bu}_8\text{N}_4\text{Ba}_2(\eta^6\text{-arene})_2]$ (arene = durene, **22**; naphthalene, **23**; toluene, **24**; benzene, **25**). The X-ray structures of **14**, **15**, **18**, **22**, and **23** are described in detail. We have tried to establish a relationship between the solid-state and solution structures by analyzing the ¹H NMR spectra of the porphyrinogen complexes.

Keywords: alkali metals • alkaline earth metals • pi interactions • porphyrinogens

Introduction

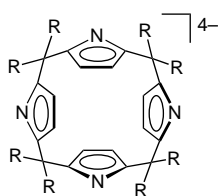
It is now clear that cation- π interactions have a prominent position among the various noncovalent binding forces that determine the solvation of metal ions.^[1] Cation- π interactions are considered in the context of biology and are involved in protein structures^[2] and protein-ligand interactions. A number of hypotheses relate the activity of artificial receptors in aqueous media^[3] with the fact that organic binding sites composed primarily of aromatic groups can compete with full aqueous solvation. The conventional assumption that the interaction of alkali cations and hard bases is energetically more favourable, has been disproved by a number of

fundamental studies which establish that cation- π interactions are among the strongest noncovalent bonding forces.^[1] Significant examples of the cation- π solvation can be found in the alkali-arylphosphane derivatives reported by G. W. Rabe et al.^[4]

This report investigates the solvation of the alkali (K, Rb, Cs) and alkaline earth ions (Ca, Sr, Ba),^[1, 5-7] with the pyrrole ring as the π binding site.^[5, 6, 8] The pyrrole ring is among the most important functionalities in natural molecules, from porphyrin to proteins, etc. The cooperative effect of four pyrroles has been considered in the form of the *meso*-octaalkylporphyrinogen tetraanion,^[8] in which each pyrrole is electronically unrelated to each other, due to the presence of *meso*-sp³ carbons. The latter assure the conformational flexibility of the porphyrinogen skeleton; thus the four pyrrolyl anions can orient to form a sort of π cavity (Scheme 1).

This arrangement of the four pyrroles, which can display an η^5 interaction both inside and outside the cavity, has been observed in a variety of transition metal derivatives.^[8] The

[a] Prof. Dr. C. Floriani, L. Bonomo, Dr. E. Solari, Dr. R. Scopelliti
Institut de Chimie Minérale et Analytique
Université de Lausanne, BCH
1015 Lausanne (Switzerland)
Fax: (+41) 21 692 3905
E-mail: carlo.floriani@icma.unil.ch



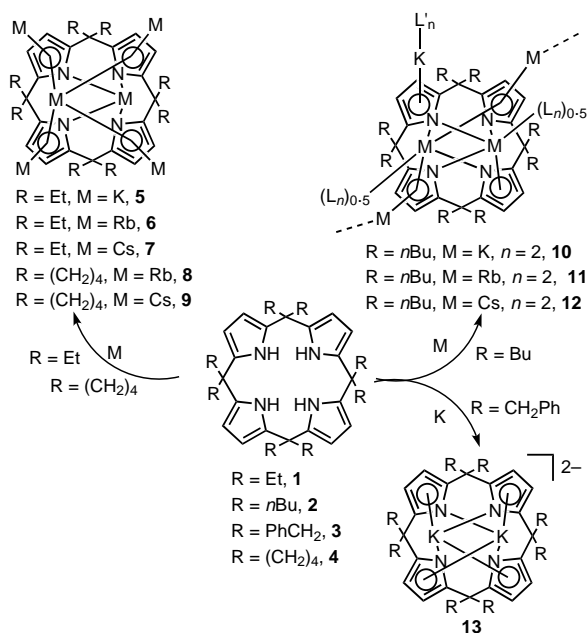
Scheme 1. The π cavity defined by the *meso*-octaalkylporphyrinogen tetraanion.

present report also presents an idea of the structural diversity that can be derived from the different bonding modes of the porphyrinogen tetraanion in the case of Group 1 and 2 metals^[9, 10] and the use of aromatic hydrocarbons as coligands^[11] to complete the coordination sphere of the alkaline earth ions. Two of the compounds reported here have appeared in a short communication.^[12]

Results and Discussion

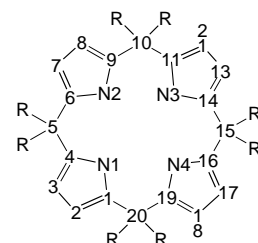
Alkali ions: K, Rb, Cs: The metallation of *meso*-octaalkylporphyrinogen with alkali metals has the double advantage of making available the deprotonated form of porphyrinogen, which is appropriate for metal complexation, and of identifying the alkali-cation bonding mode to the porphyrinogen tetraanions. There are numerous cases in which the metallo-*meso*-octaalkylporphyrinogen functions as a carrier of salts, namely alkali hydrides or polar organometallics.^[8, 13] In such compounds, the key interaction is the solvation of alkali ions by the pyrrolyl anions that function as η^3 or η^5 binding sites.^[8, 13]

By changing the size of the alkali cation, we move from monomeric structures, as observed in Li and Na derivatives,^[14, 15] to polymeric ones, as observed for K, Rb, and Cs. In the case of Cs, a significant change in the bonding mode of the alkali cation occurs, in which the π intervention with the pyrroles becomes the predominant one. The *meso* substituent at this stage become particularly important in determining both the solubility and the overall structure. The metallation of the protonated *meso*-octaalkylporphyrinogens **1–4** has been performed as reported in the Experimental Section. In the case of *meso*-ethyl or *meso*-cyclopentyl derivatives, the metallation led to polymeric unsolvated species, **5–9**, as reported in Scheme 2. With more



Scheme 2. Synthetic scheme for alkali-porphyrinogen complexes.

bulky substituents, such as the *n*-butyl, a different polymeric form comes out, with a partial solvation of the alkali cation (see complexes **10–13a**). In the case of more sterically demanding *meso* substituents, such as benzyl, the ion-separated form **13b** has been isolated. In the three classes of compounds **5–9**, **10–13a**, and **13b**, the binding of two cations inside the porphyrinogen cavity is similar. The size of the alkali cation and the *meso*-alkyl substituents are the two factors which allow one class of compounds to switch to another. The main structural features of such classes of compounds are exemplified in the structures of **7**, **10**, **13a**, and **13b**. The numbering scheme of the porphyrinogen skeleton is displayed in Scheme 3.



Scheme 3. The porphyrinogen numbering scheme.

The overall structure of the Cs-porphyrinogen **7** is a three-dimensional network (Figures 1 and 2), made up of two-dimensional sheets that are connected by solvent molecules. The two-dimensional building blocks are formed by Cs₂-porphyrinogen monomeric units connected by four Cs cations. The four pyrrolyl anions are oriented in a cone conformation, thus making a π binding cavity which hosts two Cs cations. Unlike the case of potassium (see below), the size of cesium does not allow both cesium ions to display the same bonding mode to the pyrroles. In fact, Cs1 is $\eta^1:\eta^1:\eta^1:\eta^1$ bonded to the four nitrogen atoms (Cs1...N1, 3.156(10) Å; Cs1...N2, 3.139(9) Å), while Cs2 is $\eta^5:\eta^5:\eta^5:\eta^5$ bonded to the four pyrroles and has two short and two long Cs–Pyr_{centroid} distances (Cs2– η^5 (Pyr), 3.069(8) Å, Cs2– η^5 (Pyr), 3.342(8) Å). The two Cs ions are in close proximity at 3.984(1) Å. The connectivity between the Cs₂-porphyrinogen

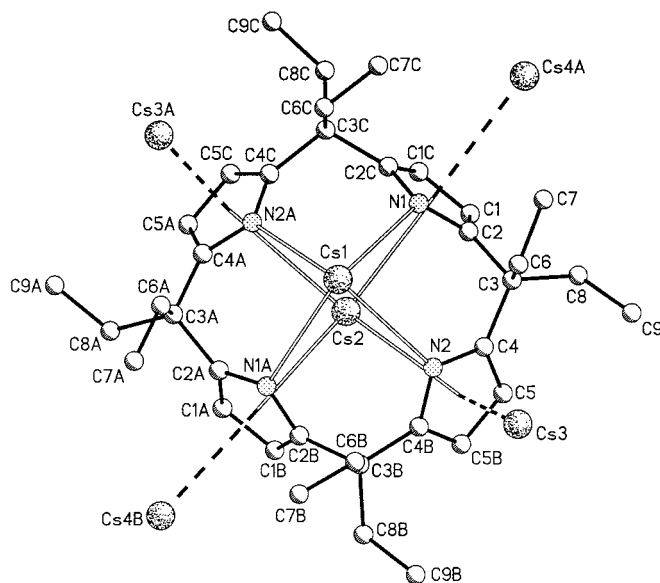
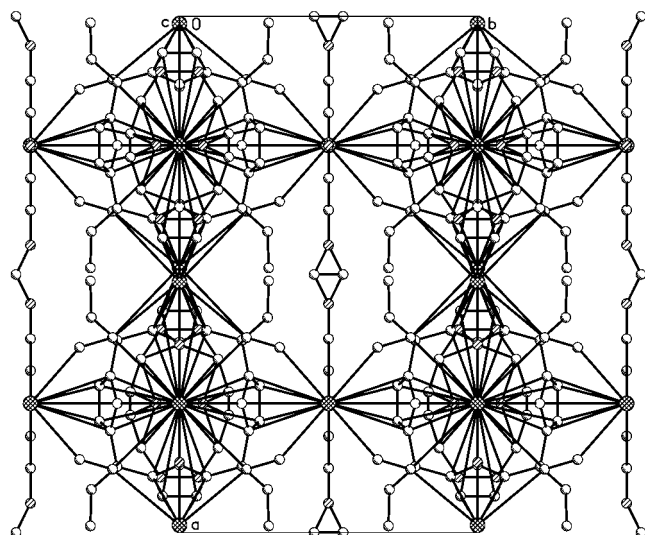
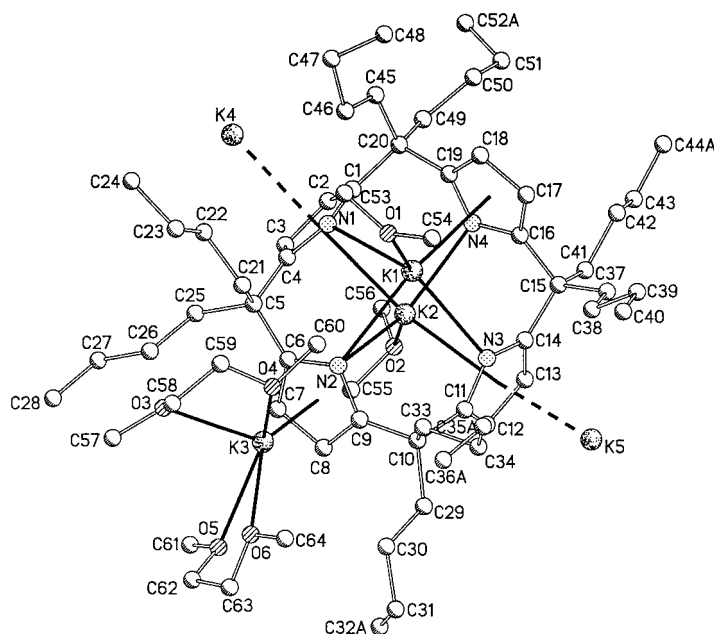


Figure 1. Ball-and-stick representation of complex **7** showing the adopted labeling scheme (solvent and hydrogen atoms omitted for clarity). Letters A, B, and C refer to the following symmetry transformations: $-x + 1/2, -y, z$; $x, -y, z$; $-x + 1/2, y, z$.

Figure 2. Crystal packing of complex **7** viewed down the *c* axis.

units is assured by the two Cs ions which are bonded η^5 to the external face of the pyrrolyl anions. The apparent large range of the Cs– η^5 (Pyr) intermolecular distances, which range from 3.107(8) to 3.330(8) Å, is due to the disorder that affects the two external Cs ions.

The molecular complexity in the solid state of the potassium derivatives **10**, **13a**, and **13b** is quite different, since it is polymeric in the first two cases and monomeric in the last. They are, however, rather close where the behavior of the porphyrinogen is concerned, acting as a π -dinucleating ligand, and the K_2 -porphyrinogen core (see Figure 3 for complex **10**). For the sake of clarity only details of **10** are given in the text, (crystallographic data for **13a** and **13b** are available from the Cambridge Crystallographic Data Centre, see Experimental Section), although we emphasize here the differences between them. The porphyrinogen skeleton displays a partial cone in **10** (Table 1), while it has a 1,3-alternate conformation in **13a** and **13b**. This difference in the conformation leads to different bonding modes of the two potassium ions inside the ligand cavity. In complex **10**, K1 is $\eta^1:\eta^1:\eta^1:\eta^5$ bonded to the four pyrroles (K1–N1 = 2.880(3), K1–N2 = 2.953(3), K1–N3 = 2.901(3), K1– η^5 (Pyr) = 2.823(2) Å), whereas K2 is $\eta^5:\eta^1:\eta^5:\eta^1$ bonded (K2(– η^5 (Pyr)) = 2.973(2), K2–N2 = 2.985(3), K2– η^5 (Pyr) = 2.910(2),

Figure 3. Ball-and-stick representation of compound **10** showing the adopted labeling scheme without the hydrogen and disordered atoms from site B.

K2–N4 = 2.812(3) Å) (Table 2). A reference compound for a structural comparison can be, among others,^[7, 16] the $[(\eta^5-C_5Me_5)KPy_2]_\infty$ (K–($\eta^5-C_5Me_5$)_{av}, 2.789; K–N_{av}, 2.926 Å).^[17] The structural parameters do not differ greatly for a wide series of cyclopentadienyl derivatives.

In the compounds **13a** and **13b** both potassium ions display the same bonding sequence $\eta^5:\eta^1:\eta^5:\eta^1$. Due to the presence of *meso*- sp^3 carbons in **1–4**, the four pyrroles adopt a parallel orientation, thus defining a π cavity, in which the two potassium ions reside (K1...K2, 3.364(1) Å in **10**). The size of the cavity is defined by the following parameters in **10**: N1...N3 = 4.922(4); N2...N4 = 4.749(4); Pyr(1)_{centroid}...Pyr(3)_{centroid}, 5.704(3); Pyr(2)_{centroid}...Pyr(4)_{centroid}, 6.223(3) Å. Complex **10** also contains, in the repeating monomeric unit, two additional potassium ions: K3, which is bonded η^5 to Pyr(2) (K–Pyr_{centroid}, 2.781(2) Å), whereas K4 and K5, which have half occupancy, bridge adjacent porphyrinogen skeletons, and give rise to a polymeric chain. K4 is located on a twofold axis and K5 on an inversion center. Both are η^5 -bonded to the pyrrolyl anions of adjacent monomeric units

Table 1. Comparison of relevant structural parameters within ligand units.

	7	10	14	15	18	19 ^[b]	22 ^[b]	23
deviations from the N ₄ core [Å]								
N1	–0.012(7)	–0.094(2)	0.095(2)	0.125(4)	0.119(7)	–0.151(1) [–0.184(1)]	0.147(9) [0.13(1)]	0.135(4)
N2	0.012(7)	0.092(2)	–0.095(2)	–0.125(4)	–0.119(7)	0.151(1) [0.184(1)]	–0.147(9) [–0.13(1)]	–0.135(4)
N3	–0.012(7)	–0.093(2)	0.095(2)	0.125(4)	0.119(7)	–0.151(1) [–0.184(1)]	0.147(9) [0.13(1)]	0.135(4)
N4	0.012(7)	0.095(2)	–0.095(2)	–0.125(4)	–0.119(7)	0.151(1) [0.184(1)]	–0.147(9) [–0.13(1)]	–0.135(4)
angle between AB ^[a] [°]	24.6(6)	102.3(2)	79.2(1)	82.2(3)	97.7(1)	83.1(1) [67.3(1)]	98.7(5) [81.4(5)]	81.3(8)
angle between AC ^[a] [°]	30.2(6)	37.7(2)	51.2(2)	43.4(3)	47.2(1)	66.5(1) [30.6(1)]	45.1(5) [43.2(5)]	135.0(8)
angle between AD ^[a] [°]	53.9(6)	95.1(2)	100.8(2)	97.8(3)	79.2(1)	66.1(1) [87.4(1)]	81.6(5) [83.1(5)]	82.0(8)
angle between BC ^[a] [°]	24.6(6)	81.9(2)	100.8(2)	97.8(3)	79.2(1)	66.1(1) [87.4(1)]	81.6(5) [97.0(5)]	81.9(8)
angle between BD ^[a] [°]	72.0(6)	13.9(2)	51.2(2)	43.4(3)	47.2(1)	30.1(1) [80.1(1)]	45.6(5) [136.8(5)]	135.0(8)
angle between CD ^[a] [°]	53.9(6)	82.6(2)	79.2(2)	82.2(3)	97.7(1)	83.1(1) [67.3(1)]	98.7(5) [98.6(5)]	81.3(8)

[a] A, B, C and D define the pyrrole rings containing N1, N2, N3 and N4 (following the labeling scheme). [b] Values in brackets refer to a second ligand unit.

Table 2. Selected bond lengths [Å] for compounds **7**, **10**, **14**, **15**, **18**, **19**, **22**, and **23**

	7 ^[b]	10 ^[b]	14	15	18	19	22	23
M1- η^5 (Pyr) ^[a]		2.823(2)	2.771(1)	2.796(2)	2.872(4)	2.581(2)	2.870(4)	2.849(6)
M2- η^5 (Pyr) ^[a]	3.069(8) [3.342(8)]	2.973(2) [2.910(2)]						
M3- η^5 (Pyr) ^[a]	3.246(8) [3.330(8)]	2.781(2)						
M4- η^5 (Pyr) ^[a]	3.107(8) [3.249(8)]	2.859(4) [2.792(2)]						
M1- η^3 (Pyr) ^[a]			2.713(1)	2.804(2)	2.882(4)		2.900(4)	2.877(6)
M1- η^1 (Pyr) ^[a]	3.156(9)	2.880(3)	2.634(2)	2.750(4)	2.843(8)	2.467(2)	2.838(8)	2.818(7)
M1- η^1 (Pyr) ^[a]	3.139(9)	2.953(3)						
M1- η^1 (Pyr) ^[a]		2.901(3)						
M2- η^1 (Pyr) ^[a]		2.985(3)						
M2- η^1 (Pyr) ^[a]		2.812(3)						
M1- η^6 (arene) ^[a]		2.812(3)					3.068(7)	3.077(7)

[a] η^5 (Pyr), η^3 (Pyr), η^1 (Pyr), η^6 (arene) indicate the centroids. [b] Values in brackets refer to different pyrrolyl moieties.

(K4–Pyr_{centroid}, 2.859(4); K5–Pyr_{centroid}, 2.792(2) Å). In addition, significant short distances have been found between the *meso*-butyl substituents and the potassium ions K4 and K5 (K4...C22 = 3.534(4); K4...C46 = 3.617(4); K5...C37 = 3.466(4); K5...C38 = 3.423(4) Å). The overall structure of **10** (Figure 3 and Figure 4) is a two-dimensional network,

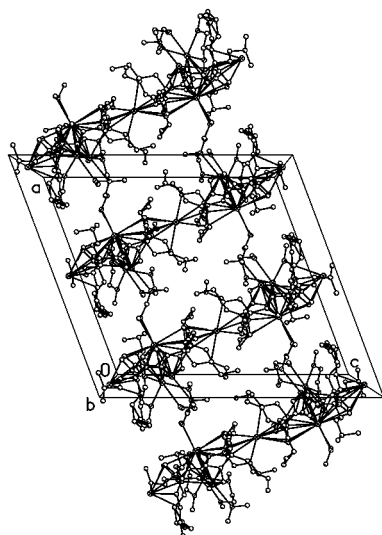


Figure 4. Crystal packing of compound **10** viewed down the *b* axis.

thanks to dimethyl ether (DME) molecules binding K1 and K2 across the polymeric chains. Complex **13a** displays a monodimensional polymeric chain arrangement similar to that found in **10**.

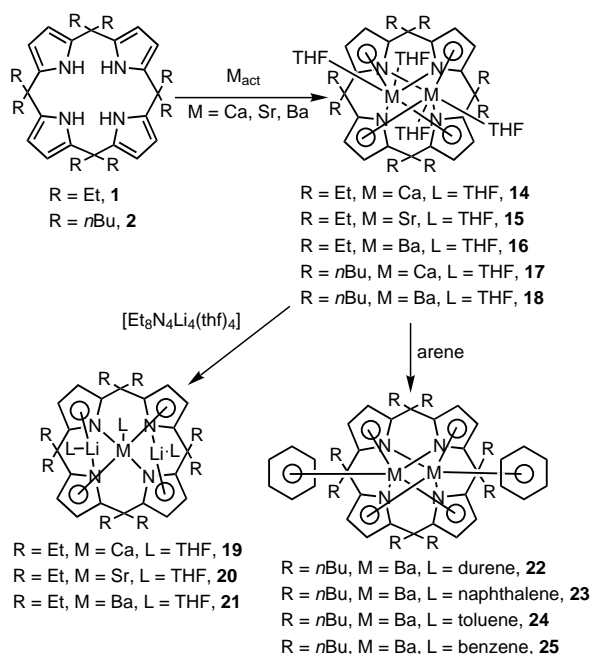
In the structural analysis of porphyrinogen alkali cation compounds, the relationship between the solid-state and solution structures is intriguing. The only method we have for inspecting the structure in solution is ¹H NMR spectroscopy. The first difficulty one faces is the insolubility of such compounds in hydrocarbons, which are the most innocent media in keeping the solid-state structure intact. When dissolved in strongly polar solvents, we expect significant modifications of the solid-state structure, although this depends on the nature of the solvent. A major difference was observed between pyridine and THF on the one hand and

dimethyl sulfoxide (DMSO) on the other. There is significant evidence that the first two solvents, though they cleave the polymeric structure, maintain the dimetallic core inside the porphyrinogen cavity, while DMSO seems to encourage partial demetallation to monometallic porphyrinogens. The ¹H NMR spectra of **6** and **7** at room temperature show a two-fold symmetry with a singlet for the eight β -pyrrole protons, while the *meso* substituents give rise to two sets of doublets of quartets and two triplets. The presence of two different ethyl groups is in agreement with the presence in the X-ray structure of two nonequivalent faces related to the N₄ mean plane, one of them containing the Cs- η^1 : η^1 : η^1 : η^1 , the other Cs- η^5 : η^5 : η^5 : η^5 . Equivalence of the ethyl groups occurs at 61 °C and 69 °C for **6** and **7**, respectively; this suggests that fluxional behavior of the two Cs ions exchanges their roles at an appropriate temperature. In the case of the potassium derivative, which has a ¹H NMR spectrum in pyridine in agreement with a fourfold symmetry at room temperature, such an exchange has a much lower thermal barrier. The ¹H NMR spectra of **5–7** in DMSO at room temperature are in agreement with a fourfold symmetry. In this latter case, the solvent causes, quite probably, a partial demetallation of the dimetallic unit, which converts it into a monometallic one, and full solvation one of the two ions of the dinuclear core.

Alkaline earth ions: Ca, Sr, Ba: In the case of the alkaline earth ions, magnesium stays *per se* due to its covalent character and its covalent radius. In fact, it forms porphyrinogen complexes in which the interactions with the ligand imply exclusive σ bonds with the N₄ core.^[18]

Ionic size is the determining factor for making the *meso*-octaalkylporphyrinogen behave mostly as π -binding systems. Therefore, we used the alkaline earth ions from calcium to barium. The metallation was carried out in THF by using the metal in an active form prepared as reported in the literature^[19] (see Experimental Section). The final compounds, complexes **14–18**, contain two metal ions squeezed inside the same cavity that are π -bonded by the pyrrolyl anions and, in addition, bind two molecules of THF (Scheme 4). The alkaline earth ion maintains the π solvation inside the porphyrinogen cavity, as do some of the early transition metal ions, namely zirconium and niobium.^[8, 14]

Complexes **14**, **15**, and **18** have quite similar structural features (Figures 5, 6, and 7). The ligand has a permanent 1,3-



Scheme 4. Synthetic scheme for porphyrinogen complexes of alkaline earth ions.

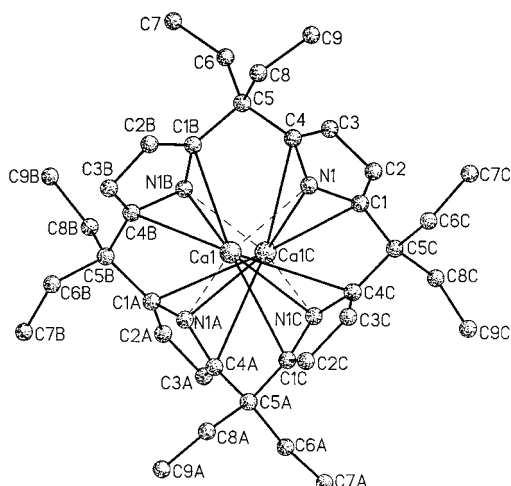


Figure 5. Ball-and-stick representation of complex **14** without hydrogens and THF molecules. Letters A, B, and C denote the following symmetry operations: $-x + 1, -y + 1/2, z$; $-y + 3/4, x - 1/4, -z + 3/4$; $y + 1/4, -x + 3/4, -z + 3/4$.

alternate conformation, thus forming a π -dinucleating cavity. The two ions are symmetrically located on opposite sides of the N_4 mean plane, and are out-of-plane by a distance of $\pm 1.621(1)$ Å for **14**, $\pm 1.736(1)$ Å for **15** and $\pm 1.856(1)$ Å for **18**. The ion size is an important factor in the determination of the bonding mode to the pyrrolyl anions. The hapticity assignment, η^3 or η^5 , is made by selecting the shortest distance of the metal to the centroid of the fragment to be considered. In many cases, a clear-cut answer is possible, while in others the two distances can be close. In complex **14**, the Ca ion may be considered as η^1 to a pair of pyrroles ($\text{Ca}-\eta^1(\text{Pyr})$, 2.634(2) Å) and η^3 to the other pairs ($\text{Ca}-\eta^3(\text{Pyr})$, 2.713(1) Å), since the calculated $\text{Ca}-\eta^5(\text{Pyr})$ distance is significantly longer ($\text{Ca}-\eta^5(\text{Pyr})$, 2.771(1) Å). In this context,

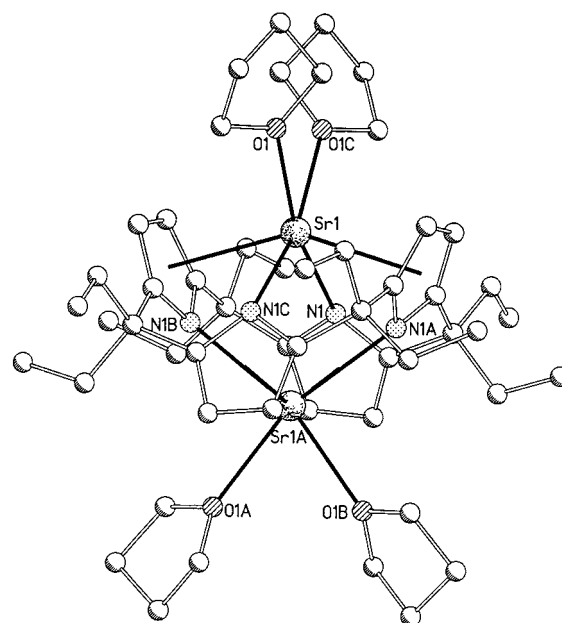


Figure 6. Ball-and-stick representation of complex **15** (hydrogens omitted for clarity). Letters A, B, and C denote the following symmetry operations: $-y + 3/4, x - 1/4, -z + 3/4$; $y + 1/4, -x + 3/4, -z + 3/4$; $-x + 1, -y + 1/2, z$.

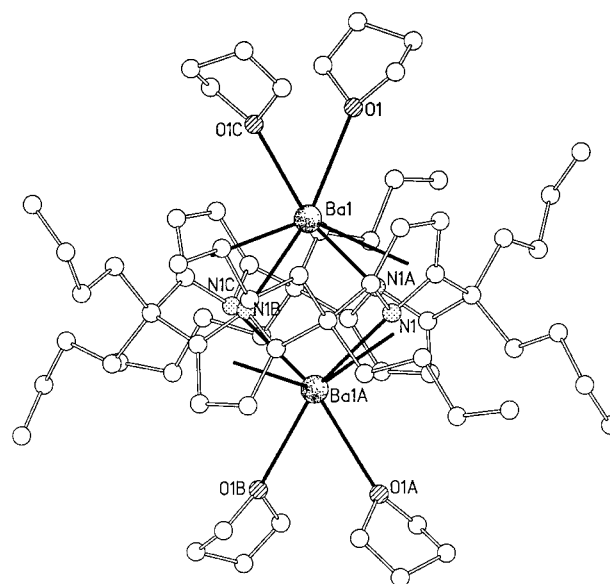


Figure 7. Ball-and-stick representation of complex **18** (hydrogens omitted for clarity). Letters A, B, and C denote the following symmetry operations: $-x + 1/4, -y + 1/4, z$; $x, -y + 1/4, -z + 1/4$; $-x + 1/4, y, -z + 1/4$.

the η^3 -bonded pyrrole may be considered as an η^3 -azaallyl, which makes an interesting structural comparison to the calcium bisallyl derivative, $[\text{Ca}\{\text{C}_3(\text{SiMe}_3)_2\text{H}_3\}_2(\text{thf})_2]^{[20]}$

By increasing the size of the cation, the ligand maintains its conformation, which is the same observed for the free form, but the cations move further away from each other ($\text{Ca} \cdots \text{Ca} = 3.241(1)$, $\text{Sr} \cdots \text{Sr} = 3.472(1)$, $\text{Ba} \cdots \text{Ba} = 3.712(1)$ Å). This move causes a change in the bonding mode of Sr and Ba, which have η^5 and η^1 interactions with the two pairs of pyrroles ($\text{Sr}-\eta^5(\text{Pyr})$, 2.796(2); $\text{Sr}-\eta^1(\text{Pyr})$, 2.750(4); $\text{Ba}-\eta^5(\text{Pyr})$, 2.872(4); $\text{Ba}-\eta^1(\text{Pyr})$, 2.843(8) Å). In complexes **15** and

18, the hapticity of the pyrrole bonding to Sr and Ba is not as clear as it is in the case of Ca, because the Sr– $\eta^3(\text{Pyr})$ and Ba– $\eta^3(\text{Pyr})$ bond lengths are 2.804(2) and 2.882(4) Å, respectively. In complexes **15** and **18** the arrangement of the two η^5 -pyrrolyl anions mimics two bent cyclopentadienyls (Pyr–M^{II}–Pyr: 148.4(1)°, 143.9(3)°, respectively). Each cation completes its coordination sphere with two THF molecules (Ca–O, 2.428(2); Sr–O, 2.578(3); Ba–O, 2.771(10) Å). These parameters are unique and cannot be compared to those of existing structures. The only possible comparison could be made with the cyclopentadienyl derivatives,^[21] although the pyrrolyl anion in a macrocyclic structure does not have the same function as the Cp ligand. In cyclopentadienyl derivatives the Ca–C bond lengths are significantly shorter, whereas in the organo-calcium compounds reported here, the average metal–carbon bond length ranges from 2.62(2) to 2.73(3) Å.^[22]

The formation of mononuclear complexes has been achieved in the reaction of **14**–**16** with the lithium-porphyrinogen, [Et₈N₄Li₄(thf)₄] which leads to **19**–**21** (Scheme 4). The reaction is, in fact, a metal redistribution reaction. The structure of **19** in Figure 8 arises formally from that of **14**, in

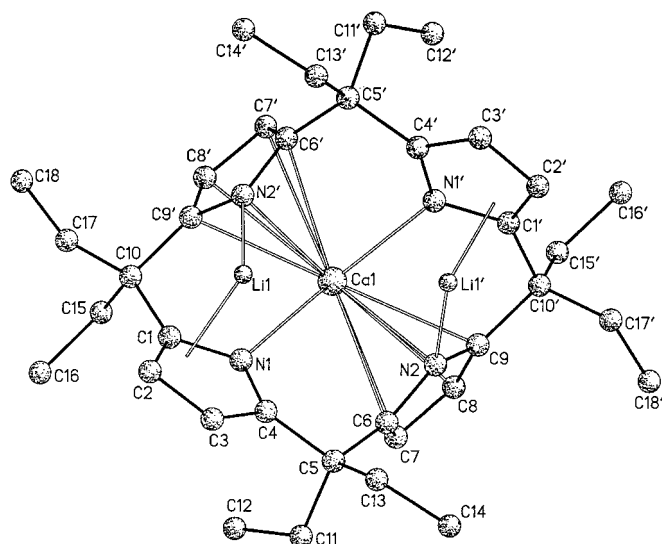


Figure 8. Ball-and-stick representation of complex **19** (hydrogens omitted for clarity). Prime denotes the following symmetry operation: $-x + 3/2, y, -z + 1/2$. Only one of the two half molecules included in the asymmetric unit is shown.

which one of the calcium cations has been replaced by two lithium cations. The calcium cation lies opposite to the two lithium cations in complex **19** with respect to the N₄ average plane (out-of-plane distances: Ca1⋯N₄ –1.256(2), Li⋯N₄ +1.635(4); and Ca2⋯N₄, +1.242(2), Li⋯N₄ –1.593(4) Å for two independent molecules). In complex **19**, which has fewer steric constraints than **14**, the calcium atom is η^5 -bonded (Ca–Pyr(centroid)_{av}, 2.581(2) Å) to the *trans*-pyrroles, which gives rise to a bent cyclopentadienyl-type structure (Pyr–Ca–Pyr, 165.95(7)°) and η^1 -bonded to the other pair of pyrroles (Ca–N_{av}, 2.467(2) Å), which in turn function as η^3 -binding sites for the two lithium cations (Li– $\eta^3(\text{N1,C1,C2})$, 2.069(5) Å).

An unusual and interesting solvation of the alkaline earth ions was observed when **18** was dissolved in isoctane in the presence of aromatic hydrocarbons. This event is shown by the formation of **22**–**25**, in which THF, which completes the coordination sphere of barium in **18**, was replaced by an arene ring. Complexes **22**–**25** have been isolated in a crystalline form and can be recrystallized from *n*-hexane. The experimental procedure shows that aromatic hydrocarbons, when used in a moderate excess, compete with THF to bind the barium cation. In addition, the chemical shift of the aromatic ring protons are significantly affected by the binding of barium, and no exchange was observed between the bound and the free aromatic hydrocarbon. Such stability and kinetic inertness is surprising for an arene-barium complex. A rare example has been reported in the literature, in which toluene is η^6 -bonded to barium (Ba–(η^6 -C₇H₈), 3.121 Å).^[23]

We give a full report on the structures of **22** and **23** in the text, while data for the analogous structures of **24** and **25** are available from the Cambridge Crystallographic Data Centre (see Experimental Section). The structures of **22** and **23** (Figures 9 and 10 respectively) are similar to that of **18**, in

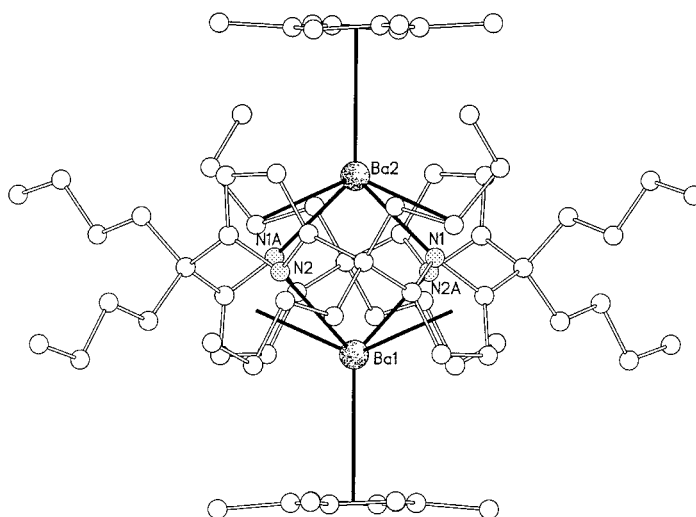


Figure 9. Ball-and-stick representation of complex **22** (hydrogens omitted for clarity). Letter A denotes the following symmetry operation: $x, -y, -z$. Only the molecule which includes Ba1 and Ba2 is shown.

which two THF molecules have been replaced by an arene ring, namely durene (**22**) and naphthalene (**23**). The ligand maintains the 1,3-alternate conformation, and the structural parameters which identify the η^5 : η^1 bonding mode of Ba to the porphyrinogen are close to those in **18** (**22**: Ba– $\eta^5(\text{Pyr})_{\text{av}}$, 2.870(4); Ba– $\eta^3(\text{Pyr})_{\text{av}}$, 2.900(4); Ba– $\eta^1(\text{Pyr})$, 2.838(8) Å. **23**: Ba– $\eta^5(\text{Pyr})_{\text{av}}$, 2.849(6); Ba– $\eta^3(\text{Pyr})_{\text{av}}$, 2.877(6); Ba– $\eta^1(\text{Pyr})$, 2.818(7) Å). The reciprocal position of the two Ba ions is slightly affected, the Ba–Ba mean distance is 3.709(1) Å in **22** and 3.694(1) Å in **23** and the out-of-N₄-plane values move to $\pm 1.855(2)$ Å and $\pm 1.847(1)$ Å in **22** and **23**, respectively. The two arene rings in **22** and **23** are η^6 -bonded to the metal with an average distance of 3.068(7) and 3.077(7) Å, respectively. The structures of **24** and **25** differentiate from those of **22** and **23** in that one barium is perfectly η^6 -bonded to the arene ring (3.068(3), 3.086(5) Å), while the other is not able to bind the

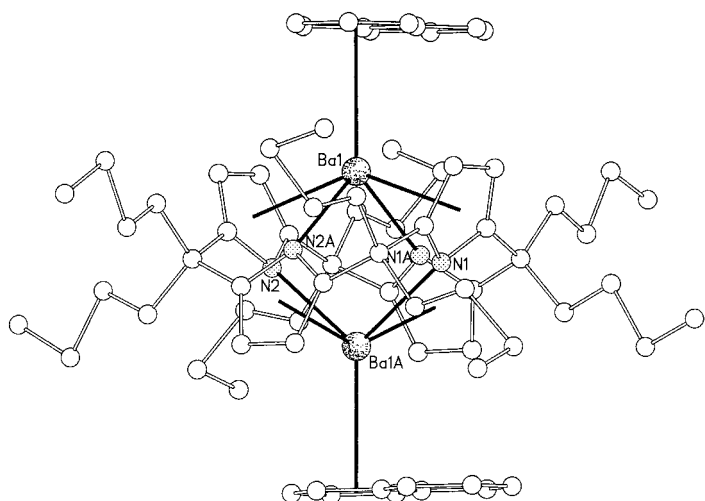


Figure 10. Ball-and-stick representation of complex **23** (hydrogens omitted for clarity). Letter A refers to the following symmetry transformation: $-x, y, -z - 1/2$.

arene ring regularly which allows only weak η^2 or η^3 bonds (η^2 for C_6H_6 , η^3 for C_7H_8).

Due to the solubility of complexes of alkaline earth ions and porphyrinogen in hydrocarbons, a close relationship between the solid-state and solution structures can be found for these complexes. The 1H NMR spectra indicate that the D_{2d} structure in the solid-state is retained in solution. The room-temperature 1H NMR spectra of **14**–**16** in toluene show a doublet of quartets and a single triplet for the *meso*-ethyl groups. Coalescence which relates to the ethyl groups is not achieved in any of those complexes at a temperature lower than $110^\circ C$. The calcium derivative **14** is near to the coalescence close to this temperature, and, as expected, its value increases with the increasing size of the metal ion. The 1H NMR spectrum of **18**, which is quite similar to those of **14**–**16**, is not particularly affected by the replacement of the two THF molecules by an arene ring in **22**–**25**. The 1H NMR spectra have a similar pattern discussed for complexes **14**–**16**.

Conclusion

This is a unique report on a macrocyclic ligand acting as π binding cavity for alkali and alkaline earth ions. In addition, it has been shown how general and relevant the π binding mode of aromatic groups can be to alkali and alkaline earth ions.^[1, 4–6] The solid-state structures have been correlated with those in solution by using 1H NMR spectroscopy. This type of structural relationship is almost neglected in the case of complexes of Group 1 and 2 metal ions.

Experimental Section

General Procedure: All operations were carried out under an atmosphere of purified nitrogen. All solvents were purified by standard methods and freshly distilled prior to use. NMR spectra were recorded on a DPX-400 Bruker instrument. Elemental analyses were performed on an EA1110CHN elemental analyzer by CE Instruments. The synthesis of **1**

was performed as reported in the literature.^[8a] The preparation of active Ca, Sr, and Ba metals was performed as reported in the literature.^[19]

Synthesis of 2: A catalytic amount of $MeSO_3H$ (4 mL) was added slowly to a stirred solution of pyrrole (50 mL, 0.72 mol) and 5-nonanone (125 mL, 0.72 mol). The solution was heated under reflux for 4 h. The white solid precipitate was collected, washed with absolute ethanol (3×200 mL), dried in vacuo, and stored under nitrogen (89.5 g, 65.0%). 1H NMR (400 MHz, $[D_6]benzene$, $25^\circ C$, TMS): $\delta = 7.09$ (brs, 4H; NH), 6.00 (d, $J(H,H) = 2.4$ Hz, 8H; C_4H_2N), 1.88 (m, 16H; CH_2), 1.5–1.2 (m, 32H; CH_2), 0.93 (t, 24H, $J(H,H) = 7.32$ Hz, CH_3); elemental analysis calcd (%) for $C_{52}H_{84}N_4$ (765.2): C 81.62, H 11.06, N 7.32; found C 81.87, H 11.13, N 7.35.

Synthesis of 3: A catalytic amount of $MeSO_3H$ (1 mL) was added to a solution of dibenzylketone (21.0 g, 0.1 mol) and pyrrole (7 mL, 0.1 mol) in MeOH (300 mL). The reaction mixture was refluxed for 12 h. A white precipitate was collected, washed with acetone (2×25 mL) and dried in vacuo (8 g, 32%). Crystals suitable for X-ray diffraction were grown in a mixture of THF/*n*-hexane. 1H NMR (CD_2Cl_2 , 400 MHz, $[D_2]dichloromethane$, $25^\circ C$, TMS): $\delta = 7.20$ (m, 24H; ArH), 6.90 (m, 16H; ArH), 6.27 (brs, 4H; NH), 5.65 (d, $J(H,H) = 2.4$ Hz, 8H; C_4H_2N), 2.90 (q, $J(H,H) = 12.7$ Hz, 16H; CH_2); elemental analysis calcd (%) for $C_{76}H_{68}N_4$ (1037.4): C 87.99, H 6.61, N 5.40; found C 87.13, H 7.17, N 5.41.

Synthesis of 4: $MeSO_3H$ (5 mL) was added slowly to a solution of cyclopentanone (100 mL, 1.25 mol) and pyrrole (87 mL, 1.25 mol) in EtOH (800 mL). The reaction mixture was refluxed for 3 h. The white solid precipitate was collected, washed with EtOH (4×100 mL), and dried in vacuo (110 g, 66%). Crystals suitable for X-ray diffraction were grown in a mixture of THF/*n*-hexane. 1H NMR (400 MHz, $[D_2]dichloromethane$, $25^\circ C$, TMS): $\delta = 7.10$ (brs, 4H; NH), 5.89 (d, $J(H,H) = 2.9$ Hz, 8H; C_4H_2N), 2.04 (m, 16H; CH_2), 1.71 (m, 16H; CH_2); elemental analysis calcd (%) for $C_{36}H_{44}N_4$ (532.8): C 81.16, H 8.32, N 10.52; found C 80.93, H 8.38, N 10.54.

Synthesis of 5: Potassium (26.6 g, 0.68 mol) and naphthalene (43.6 g, 0.340 mol) were added to a solution of **1** (92 g, 0.17 mol) in THF (800 mL) at room temperature. The reaction mixture was heated under reflux for several days. Once the reaction was completed, a white solid dried in vacuo (99 g, 84%). 1H NMR (400 MHz, $[D_6]DMSO$, $25^\circ C$, TMS): $\delta = 5.20$ (s, 8H; C_4H_2N), 1.67 (q, $J(H,H) = 7.34$ Hz, 16H; CH_2), 0.38 (t, $J(H,H) = 7.34$ Hz, 24H; CH_3); 1H NMR ($[D_5]pyridine$, 400 MHz, 298 K, TMS): $\delta = 5.54$ (s, 8H; C_4H_2N), 1.82 (q, $J(H,H) = 7.34$ Hz, 16H; CH_2), 0.53 (t, $J(H,H) = 7.34$ Hz, 24H; CH_3); elemental analysis calcd (%) for $C_{36}H_{48}K_4N_4$ (693.2): C 62.38, H 6.98, N 8.08; found C 62.52, H 6.62, N 8.11.

Synthesis of 6: Rubidium (0.93 g, 10.9 mmol) and naphthalene (0.7 g, 5.45 mol) were added to a solution of **1** (1.47 g, 2.72 mmol) in THF (100 mL) at room temperature. The reaction mixture was heated under reflux for several days. Once the rubidium was eliminated, the white precipitate was collected and dried in vacuo (1.7 g, 71%). 1H NMR (400 MHz, $[D_6]DMSO$, $25^\circ C$, TMS): $\delta = 5.17$ (s, 8H; C_4H_2N), 1.63 (q, $J(H,H) = 7.34$ Hz, 16H; CH_2), 0.34 (t, $J(H,H) = 7.34$ Hz, 24H; CH_3); 1H NMR (400 MHz, $[D_5]pyridine$, $25^\circ C$, TMS): $\delta = 6.25$ (s, 8H; C_4H_2N), 2.56 (dq, $J_{gem}(H,H) = 13.2$ Hz, $J_{vic}(H,H) = 7.34$ Hz, 4H; CH_2), 2.44 (dq, $J_{gem}(H,H) = 13.2$ Hz, $J_{vic}(H,H) = 7.34$ Hz, 4H; CH_2), 2.28 (dq, $J_{gem}(H,H) = 13.2$ Hz, $J_{vic}(H,H) = 7.34$ Hz, 4H; CH_2), 2.1 (dq, $J_{gem}(H,H) = 13.2$ Hz, $J_{vic}(H,H) = 7.34$ Hz, 4H; CH_2), 1.04 (t, $J(H,H) = 7.34$ Hz, 12H; CH_3), 0.84 (t, $J(H,H) = 7.34$ Hz, 12H; CH_3); 1H NMR (400 MHz, $[D_5]pyridine$, $87^\circ C$, TMS): $\delta = 5.74$ (s, 8H; C_4H_2N), 2.26 (q, $J(H,H) = 7.34$ Hz, 16H; CH_2), 0.34 (t, $J(H,H) = 7.34$ Hz, 24H; CH_3); elemental analysis calcd (%) for $C_{36}H_{48}N_4Rb_4$ (878.7): C 49.21, H 5.51, N 6.38; found C 49.34, H 5.67, N 6.47.

Synthesis of 7: Cesium (0.98 g, 7.39 mmol) and naphthalene (0.47 g, 3.7 mmol) were added to a solution of **1** (1.0 g, 1.85 mmol) in THF (100 mL) at room temperature. The reaction mixture was heated under reflux overnight. The white precipitate was collected and dried in vacuo (1.6 g, 81%). 1H NMR (400 MHz, $[D_6]DMSO$, $25^\circ C$, TMS): $\delta = 5.17$ (s, 8H; C_4H_2N), 1.63 (q, $J(H,H) = 7.34$ Hz, 16H; CH_2), 0.34 (t, $J(H,H) = 7.34$ Hz, 24H; CH_3); 1H NMR (400 MHz, $[D_5]pyridine$, $25^\circ C$, TMS): $\delta = 6.19$ (s, 8H; C_4H_2N), 2.42 (dq, $J_{gem}(H,H) = 13.2$ Hz, $J_{vic}(H,H) = 7.34$ Hz, 4H; CH_2), 2.36 (dq, $J_{gem}(H,H) = 13.2$ Hz, $J_{vic}(H,H) = 7.34$ Hz, 4H; CH_2), 2.22 (dq, $J_{gem}(H,H) = 13.2$ Hz, $J_{vic}(H,H) = 7.34$ Hz, 4H; CH_2), 2.05 (dq, $J_{gem}(H,H) = 13.2$ Hz, $J_{vic}(H,H) = 7.34$ Hz, 4H; CH_2), 1.12 (t, $J(H,H) = 7.34$ Hz, 12H; CH_3), 0.87 (t, $J(H,H) = 7.34$ Hz, 12H; CH_3); 1H NMR (400 MHz, $[D_5]pyridine$, $87^\circ C$, TMS): $\delta = 5.83$ (s, 8H; C_4H_2N), 2.15 (brs, 16H; CH_2), 0.28 (t, $J(H,H) = 7.34$ Hz, 24H; CH_3); elemental analysis calcd

(%) for $C_{36}H_{48}Cs_4N_4$ (1068.4): C 40.47, H 4.53, N 5.24; found C 40.78, H 4.62, N 5.37; X-ray analysis was performed on the solvated form of **7**, which was recrystallized from diglyme, [**7**(Digly)₂].

Synthesis of 8: Rubidium (0.5 g, 5.85 mmol) and naphthalene (0.37 g, 2.92 mmol) were added to a solution of **4** (0.78 g, 1.46 mmol) in THF (100 mL) at room temperature. The reaction mixture was heated under reflux overnight. The white precipitate was collected and dried in vacuo (1.1 g, 86%). ¹H NMR (400 MHz, [D₆]DMSO, 25 °C, TMS): δ = 5.15 (s, 8H; C₄H₂N), 1.91 (t, *J*(H,H) = 6.85 Hz, 16H; CH₂), 1.38 (t, *J*(H,H) = 6.85 Hz, 16H; CH₂); elemental analysis calcd (%) for C₃₆H₄₀N₄Rb₄ (870.6): C 49.67, H 4.63, N 6.43; found C 49.60, H 4.52, N 6.12.

Synthesis of 9: Cesium (1.0 g, 8.28 mmol) and naphthalene (0.53 g, 4.14 mmol) were added to a solution of **4** (1.1 g, 2.07 mmol) in THF (100 mL) at room temperature. The reaction mixture was heated under reflux overnight. A white precipitate was collected and dried in vacuo (1.7 g, 77%). ¹H NMR (400 MHz, [D₆]DMSO, 25 °C, TMS): δ = 5.05 (s, 8H; C₄H₂N), 2.07 (t, *J*(H,H) = 6.85 Hz, 16H; CH₂), 1.39 (t, *J*(H,H) = 6.85 Hz, 16H; CH₂); elemental analysis calcd (%) for C₃₆H₄₀Cs₄N₄ (1060.3): C 40.78, H 3.80, N 5.28; found C 40.83, H 3.91, N 5.02.

Synthesis of 10: Potassium (2.64 g, 68.0 mmol) and naphthalene (4.33 g, 34.0 mmol) were to a solution of **2** (12.9 g, 17.0 mmol) in THF (300 mL) added at room temperature. The reaction mixture was heated under reflux for several days. Once the potassium was eliminated, a white solid was collected and dried in vacuo (13.8 g, 72%). ¹H NMR (200 MHz, [D₆]DMSO, 25 °C, TMS): δ = 5.14 (s, 8H; C₄H₂N), 3.55 (m, 16H; THF), 1.75 (m, 16H; THF), 1.68 (m, 16H; CH₂), 0.98 (m, 16H; CH₂), 0.81 (m, 16H; CH₂), 0.68 (t, *J*(H,H) = 7.34 Hz, 24H; CH₃); elemental analysis calcd (%) for C₅₂H₈₀K₄N₄·4THF (1206.0): C 67.72, H 9.36, N 4.65; found C 68.39, H 9.35, N 4.76. The X-ray analysis was performed on the DME solvated form of **10** (**10**·3DME).

Synthesis of 11: Rubidium (0.89 g, 10.44 mmol) and naphthalene (0.67 g, 5.2 mmol) were added to a solution of **2** (2.0 g, 2.61 mmol) in THF (100 mL) at room temperature. The reaction mixture was heated under reflux for 12 h. A white precipitate was collected and dried in vacuo (2.5 g, 69%). ¹H NMR (400 MHz, [D₆]DMSO, 25 °C, TMS): δ = 5.11 (s, 8H; C₄H₂N), 3.55 (m, 16H; THF), 1.71 (m, 16H; THF), 1.61 (m, 16H; CH₂), 0.95 (m, 16H; CH₂), 0.83 (m, 16H; CH₂), 0.64 (t, *J*(H,H) = 7.34 Hz, 24H; CH₃); elemental analysis calcd (%) for C₅₂H₈₀N₄Rb₄·4THF (1391.5): C 58.69, H 8.11, N 4.03; found C 58.09, H 7.85, N 4.26.

Synthesis of 12: Cesium (1.39 g, 10.44 mmol) and naphthalene (0.67 g, 5.22 mmol) were added to a solution of **2** (2.0 g, 2.61 mmol) in THF (100 mL) at room temperature. The reaction mixture was refluxed overnight. A white solid was collected and dried in vacuo (2.8 g, 68%). ¹H NMR (400 MHz, [D₆]DMSO, 25 °C, TMS): δ = 5.12 (s, 8H; C₄H₂N), 3.55 (m, 16H; THF), 1.71 (m, 16H; THF), 1.62 (m, 16H; CH₂), 1.0 (m, 16H; CH₂ overlapping with m, 16H; CH₂), 0.68 (t, *J*(H,H) = 7.34 Hz, 24H; CH₃); elemental analysis calcd (%) for C₅₂H₈₀Cs₄N₄·4THF (1581.3): C 51.65, H 7.14, N 3.54; found C 51.18, H 6.97, N 3.69.

Synthesis of 13: Potassium (2.64 g, 68.0 mmol) and naphthalene (4.33 g, 34.0 mmol) were added to a solution of **3** (12.9 g, 17.0 mmol) in THF (300 mL) at room temperature. The reaction mixture was heated under reflux for several days. Once the potassium was eliminated, a white solid was collected and dried in vacuo (13.8 g, 61%). ¹H NMR (400 MHz, [D₈]THF, 25 °C, TMS): δ = 7.12 (m, 16H; ArH), 6.96 (brs, 8H; ArH), 6.84 (m, 16H; ArH), 5.89 (s, 8H; C₄H₂N), 3.58 (m, 8H; THF), 3.08 (brs, 8H; CH₂), 3.03 (brs, 8H; CH₂), 1.58 (m, 8H; THF); elemental analysis calcd (%) for C₇₆H₆₄K₄N₄·2THF (1333.9): C 75.63, H 6.05, N 4.20; found C 76.04, H 6.12, N 4.25; X-ray analysis was performed on two differently solvated forms: **13a** = [**13**(thf)₅]·THF and **13b** = [**13**][K(Digly)₂].

Synthesis of 14: A suspension of active calcium^[19] (27.7 mmol) in THF (300 mL) was added to a solution of **1** (7.03 g, 13.0 mmol) in THF (200 mL), and the reaction mixture was stirred for 1 h at room temperature. The white suspension, which formed rapidly, was stirred for 2 h, and then the solvent was evaporated to dryness. The solid residue was extracted with benzene (250 mL), and the solution was evaporated to dryness. The residue was triturated with *n*-hexane (200 mL) to give a white solid that was collected and dried in vacuo (8.55 g, 72.6%). Crystals of **14** suitable for X-ray analysis were grown in a mixture of THF/*n*-hexane and contain a THF molecule of crystallization. ¹H NMR (400 MHz, [D₈]toluene, 25 °C, TMS): δ = 6.11 (s, 8H; C₄H₂N), 3.45 (m, 16H; THF), 2.14 (dq, *J*_{gem}(H,H) = 14.2 Hz,

*J*_{vic}(H,H) = 7.34 Hz, 8H; CH₂), 2.2 (dq, *J*_{gem}(H,H) = 14.2 Hz, *J*_{vic}(H,H) = 7.34 Hz, 8H; CH₂), 1.29 (m, 16H; THF), 0.85 (t, *J*(H,H) = 7.32 Hz, 24H; CH₃); elemental analysis calcd (%) for C₅₂H₈₀N₄Ca₂O₄ (905.4): C 68.98, H 8.91, N 6.19; found C 68.44, H 8.82, N 6.11.

Synthesis of 15: Compound **1** (7.6 g, 14.1 mmol) was added to a suspension of active strontium (28.2 mmol) in THF (300 mL). The reaction mixture was stirred for 5 h at room temperature. The solvent was evaporated to dryness. The solid residue was extracted with benzene (250 mL), and the solution was evaporated to dryness. *n*-Hexane (200 mL) was added and gave rise to a white solid that was collected and dried in vacuo (10.23 g, 72.5%). Crystals suitable for X-ray analysis were grown in a mixture of THF/*n*-hexane and contain one THF of crystallization. ¹H NMR (400 MHz, [D₈]toluene, 25 °C, TMS): δ = 6.07 (s, 8H; C₄H₂N), 3.45 (m, 16H; THF), 2.21 (dq, *J*_{gem}(H,H) = 14.2 Hz, *J*_{vic}(H,H) = 7.34 Hz, 8H; CH₂), 2.0 (dq, *J*_{gem}(H,H) = 14.2 Hz, *J*_{vic}(H,H) = 7.34 Hz, 8H; CH₂), 1.29 (m, 16H; THF), 0.9 (t, *J*(H,H) = 7.32 Hz, 24H; CH₃); elemental analysis calcd for C₅₂H₈₀N₄Sr₂ (1000.5): C 62.43, H 8.06, N 5.60; found C 62.53, H 8.12, N 6.01.

Synthesis of 16: Compound **1** (2.93 g, 5.4 mmol) was added to a suspension of active barium (10.8 mmol) in THF (300 mL), and the reaction mixture was stirred overnight at room temperature. The solvent was evaporated to dryness, the solid residue was extracted with benzene (100 mL), and the resulting solution was evaporated to dryness. The residue was triturated with *n*-hexane (80 mL) to give a white solid that was collected and dried in vacuo (3.93 g, 66%). ¹H NMR (400 MHz, [D₈]toluene, 25 °C, TMS): δ = 5.88 (s, 8H; C₄H₂N), 3.76 (m, 16H; THF), 2.12 (dq, *J*_{gem}(H,H) = 14.2 Hz, *J*_{vic}(H,H) = 7.34 Hz, 8H; CH₂), 1.73 (dq, *J*_{gem}(H,H) = 14.2 Hz, *J*_{vic}(H,H) = 7.34 Hz, 8H; CH₂), 1.44 (m, 16H; THF), 0.83 (t, *J*(H,H) = 7.34 Hz, 24H; CH₃); elemental analysis calcd (%) for C₅₂H₈₀Ba₂N₄O₄ (1099.9): C 56.79, H 7.33, N 5.09; found C 56.36, H 7.12, N 4.88.

Synthesis of 17: A suspension of active calcium (26.0 mmol) in THF (300 mL) was added to a solution of **2** (10 g, 13.0 mmol) in THF (200 mL), and the reaction mixture was stirred for 12 h at room temperature. The solvent was evaporated to dryness and benzene (250 mL) was added. Undissolved NaI was filtered off. The solution was evaporated to dryness, and *n*-pentane (100 mL) was added to give a white solid that was collected and dried in vacuo (9.35 g, 64%). ¹H NMR (400 MHz, [D₈]toluene, 25 °C, TMS): δ = 6.11 (s, 8H; C₄H₂N), 3.93 (m, 16H; THF), 2.25 (ddd, *J*_{gem}(H,H) = 13.2 Hz, *J*_{vic1}(H,H) = 12.2 Hz, *J*_{vic2}(H,H) = 3.9 Hz, 8H; CH₂), 1.93 (ddd, *J*_{gem}(H,H) = 13.2 Hz, *J*_{vic1}(H,H) = 12.2 Hz, *J*_{vic2}(H,H) = 3.9 Hz, 8H; CH₂), 1.6–1.5 (m, 24H; CH₂), 1.32 (m, 16H; THF), 1.19 (m, 8H; CH₂), 1.04 (t, *J*(H,H) = 7.34 Hz, 24H; CH₃); elemental analysis calcd for C₆₈H₁₁₂Ca₂N₄O₄ (1129.8): C 72.29, H 9.99, N 4.96; found C 72.54, H 9.69, N 4.87.

Synthesis of 18, 24, and 25: A suspension of active barium (36.0 mmol) in THF (300 mL) was added to a solution of **2** (13.8 g, 18.0 mmol) in THF (200 mL), and the reaction mixture was stirred for 12 h at room temperature. The solvent was evaporated to dryness, and benzene (250 mL) was added. Undissolved NaI was filtered off. The solution was evaporated to dryness, and *n*-pentane (100 mL) was added to give a white solid, which was collected and dried in vacuo (15.6 g, 65%). Crystals suitable for X-ray analysis were obtained from hot isoctane.

Compound 18: ¹H NMR (400 MHz, [D₈]toluene, 25 °C, TMS): δ = 5.92 (s, 8H; C₄H₂N), 3.54 (m, 16H; THF), 2.20 (ddd, *J*_{gem}(H,H) = 13.2 Hz, *J*_{vic1}(H,H) = 12.2 Hz, *J*_{vic2}(H,H) = 3.9 Hz, 8H; CH₂), 1.73 (ddd, *J*_{gem}(H,H) = 13.2 Hz, *J*_{vic1}(H,H) = 12.2 Hz, *J*_{vic2}(H,H) = 3.9 Hz, 8H; CH₂), 1.5–1.3 (m, 16H; THF + m, 24H; CH₂), 1.16 (m, 8H; CH₂), 1.33 (m, 16H; THF), 1.03 (t, *J*(H,H) = 7.34 Hz, 24H; CH₃); elemental analysis calcd (%) for C₆₈H₁₁₂Ba₂N₄O₄ (1324.3): C 61.67, H 8.52, N 4.23; found C 61.48, H 8.63, N 4.10.

Compound 25: Compound **18** was heated under reflux in benzene to produce **25**, a white crystalline solid; elemental analysis calcd (%) for C₆₂H₉₂Ba₂N₄ (1192.1): C 64.48, H 7.78, N 4.70; found C 64.37, H 7.63, N 4.55. Crystals suitable for X-ray analysis contained two molecules of benzene of crystallization.

Compound 24: Compound **18** was heated under reflux in toluene gave crystals suitable for X-ray analysis which corresponded to compound **24**; elemental analysis calcd (%) for **24**, C₆₆H₉₆Ba₂N₄ (1220.1): C 64.97, H 7.93, N 4.59; found C 64.63, H 8.12, N 4.23. The crystals used for the X-ray analysis contained two moles of C₇H₈ as crystallization solvent.

Synthesis of 19: A solution of $[\text{Et}_8\text{N}_4\text{Li}_4(\text{thf})_4]$ (3.22 g, 3.8 mmol) and **14** (3.44 g, 3.8 mmol) in THF (300 mL) was heated under reflux for 24 h. The solution was evaporated to dryness and the white residue was triturated with *n*-hexane to give a white solid, which was collected and dried in vacuo (2.76 g, 85.0%). Crystals suitable for X-ray analysis were grown in a mixture of THF/*n*-hexane. ^1H NMR (400 MHz, $[\text{D}_6]$ benzene, 25 °C, TMS): δ = 6.18 (s, 8H; $\text{C}_4\text{H}_2\text{N}$), 3.44 (m, 16H; THF), 2.06 (q, $J(\text{H,H})$ = 7.32 Hz, 8H; CH_2), 2.00 (q, $J(\text{H,H})$ = 7.32 Hz, 8H; CH_2), 1.34 (m, 16H; THF), 1.00 (t, $J(\text{H,H})$ = 7.32 Hz, 12H; CH_3), 0.94 (t, $J(\text{H,H})$ = 7.32 Hz, 12H; CH_3); elemental analysis calcd (%) for $\text{C}_{52}\text{H}_{80}\text{N}_4\text{CaLi}_2\text{O}_4$ (879.2): calcd C 71.04, H 9.17, N 6.37; found C 71.07, H 9.01, N 6.90.

Synthesis of 20: A solution of $[\text{Et}_8\text{N}_4\text{Li}_4(\text{thf})_4]$ (4.0 g, 4.69 mmol) and **15** (4.69 g, 4.69 mmol) in THF (300 mL) was heated under reflux for 24 h. The solution was evaporated to dryness and the white residue was triturated with *n*-hexane to give a white solid, which was collected and dried in vacuo (6.2 g, 71%). ^1H NMR (400 MHz, $[\text{D}_8]$ toluene, 25 °C, TMS): δ = 6.13 (s, 8H; $\text{C}_4\text{H}_2\text{N}$), 3.25 (m, 16H; THF), 2.20 (q, $J(\text{H,H})$ = 7.32 Hz, 8H; CH_2), 2.06 (q, $J(\text{H,H})$ = 7.32 Hz, 8H; CH_2), 1.31 (m, 16H; THF), 1.07 (t, $J(\text{H,H})$ = 7.32 Hz, 12H; CH_3), 0.97 (t, $J(\text{H,H})$ = 7.32 Hz, 12H; CH_3); elemental analysis calcd (%) for $\text{C}_{55}\text{H}_{80}\text{Li}_2\text{N}_4\text{O}_4\text{Sr}$ (926.7): C 67.39, H 8.70, N 6.05; found C 67.56, H 9.0, N 5.88.

Synthesis of 21: A solution of $[\text{Et}_8\text{N}_4\text{Li}_4(\text{thf})_4]$ (3.5 g, 3.8 mmol) and **16** (4.52 g, 4.11 mmol) in THF (300 mL) was heated under reflux for 24 h. The solution was evaporated to dryness and the white residue was triturated with *n*-hexane to give a white solid, which was collected and dried in vacuo (5.12 g, 69.0%). ^1H NMR (400 MHz, $[\text{D}_8]$ toluene, 25 °C, TMS): δ = 6.00 (s, 8H; $\text{C}_4\text{H}_2\text{N}$), 3.25 (m, 16H; THF), 2.12 (q, $J(\text{H,H})$ = 7.32 Hz, 8H; CH_2), 1.92 (q, $J(\text{H,H})$ = 7.32 Hz, 8H; CH_2), 1.32 (m, 16H; THF), 1.11 (t, $J(\text{H,H})$ = 7.32 Hz, 12H; CH_3), 0.87 (t, $J(\text{H,H})$ = 7.32 Hz, 12H; CH_3); elemental analysis calcd (%) for $\text{C}_{52}\text{H}_{80}\text{BaLi}_2\text{N}_4\text{O}_4$ (976.4): C 63.96, H 8.26, N 5.74; found C 63.54, H 7.95, N 5.35.

Synthesis of 22: A solution of **18** (3.0 g, 2.26 mmol) and durene (1.2 g, 9.0 mmol) was heated under reflux for 24 h in isooctane. After cooling, a white crystalline solid precipitated was collected and dried in vacuo (1.2 g, 41%). Crystals suitable for X-ray diffraction were obtained from isooctane. ^1H NMR (400 MHz, $[\text{D}_8]$ toluene, 25 °C, TMS): δ = 6.85 (s, 4H; ArH), 5.85 (s, 8H; $\text{C}_4\text{H}_2\text{N}$), 2.15 (ddd, $J_{\text{gem}}(\text{H,H})$ = 13.2 Hz, $J_{\text{vic1}}(\text{H,H})$ = 12.2 Hz, $J_{\text{vic2}}(\text{H,H})$ = 3.9 Hz, 8H; CH_2), 2.11 (s, 24H; CH_3), 1.69 (ddd, $J_{\text{gem}}(\text{H,H})$ = 13.2 Hz, $J_{\text{vic1}}(\text{H,H})$ = 12.2 Hz, $J_{\text{vic2}}(\text{H,H})$ = 3.9 Hz, 8H; CH_2), 1.55–1.3 (m, 24H; CH_2), 1.01 (m, 8H; CH_2), 1.04 (t, $J(\text{H,H})$ = 7.32 Hz, 24H; CH_3); elemental analysis calcd (%) for $\text{C}_{72}\text{H}_{108}\text{Ba}_2\text{N}_4$ (1304.3): C 66.3, H 8.35, N 4.30; found C 66.18, H 8.12, N 4.06.

Synthesis of 23: A solution of **18** (5.0 g, 3.77 mmol) and naphthalene (1.9 g, 15.1 mmol) was heated under reflux in isooctane for 24 h. After cooling, a white crystalline precipitate was collected and dried in vacuo (2.9 g, 59%). Crystals suitable for X-ray analysis were obtained from *n*-hexane. ^1H NMR (400 MHz, $[\text{D}_6]$ benzene, 25 °C, TMS): δ = 7.71 (m, 8H; ArH), 7.17 (m, 8H; ArH), 5.98 (s, 8H; $\text{C}_4\text{H}_2\text{N}$), 2.26 (ddd, $J_{\text{gem}}(\text{H,H})$ = 13.2 Hz, $J_{\text{vic1}}(\text{H,H})$ = 12.2 Hz, $J_{\text{vic2}}(\text{H,H})$ = 3.9 Hz, 8H; CH_2), 1.78 (ddd, $J_{\text{gem}}(\text{H,H})$ = 13.2 Hz, $J_{\text{vic1}}(\text{H,H})$ = 12.2 Hz, $J_{\text{vic2}}(\text{H,H})$ = 3.9 Hz, 8H; CH_2), 1.42 (m, 24H; CH_2), 1.22 (m, 8H; CH_2), 1.04 (t, $J(\text{H,H})$ = 7.32 Hz, 24H; CH_3); elemental analysis calcd (%) for $\text{C}_{72}\text{H}_{96}\text{Ba}_2\text{N}_4$ (1292.2): C 66.92, H 7.49, N 4.34; found C 66.98, H 7.81, N 4.14.

X-ray crystallography: Suitable crystals of compounds **7**, **10**, **14**, **15**, **18**, **19**, **22**, and **23** were mounted in glass capillaries and sealed under nitrogen. Crystallographic data is listed in Table 3. Data for complexes **15**, **18**, **22**, and **23** were collected at 143 K on a mar 345 imaging plate detector and reduced with marHKL release 1.9.1.^[24] Diffraction data for compounds **7**, **10**, **14**, and **19** were collected at 143 K on a KUMA diffractometer, which has *k* geometry, equipped with a CCD area detector and reduced with CrysAlis RED release 1.6.3.^[25] No absorption corrections were made for any of the data sets. Structure solutions were determined with SIR97.^[26] All structures were refined using the full-matrix least-squares on F^2 with all non-H atoms anisotropically defined. The H atoms were placed in calculated positions by using the “riding model” with $U_{\text{iso}} = a \times U_{\text{eq}}(\text{C})$ (where *a* is 1.5 for methyl hydrogens and 1.2 for other hydrogens, while C is the parent carbon atom). All structures (except **19**) were problematic to refine and the strategies we used to work them out are listed below.

The external cesium ions and solvent molecules of compound **7** were disordered. For example, although CS3 lies on a *m* symmetry site; its

occupancy factor was forced to be ¼. Cs4 was split in two positions, A and B, over a *mm2* symmetry site; this forced their overall occupancy factors [$A = 0.145(2)$, $B = 0.106(2)$] to be equal to ¼ (by means of the SUMP instruction). These problems that concerned the cesiums also affected the solvent molecules, which were retained as isotropic and geometrically restrained and for which it was not possible to locate all the atoms. Hydrogens belonging to such molecules were not included in the model.

Compound **10** showed disorder that involved terminal atoms of the *n*-butyl chains of the ligand (atoms C32, C35, C36, C44, and C52). It was possible, in this case, to find two different sites, A and B, in which their occupancy factors could be constrained to 1 by means of the PART instruction (occupancy factors for site A: C32 (0.77(1)), C35 and C36 (0.76(2)), C44 (0.62(1)), C52 (0.81(1)). These disordered parts of the structure model required geometric and rigid-body restraints to obtain acceptable thermal and geometrical parameters.

The problems encountered in compounds **14** and **15** refer to the external THF molecule which was disordered; this was complicated by symmetry. No hydrogens belonging to the disordered THF molecule were included in the model, and some geometrical restraints were applied.

In the case of complex **18**, the atoms showed very high vibrational motion and rigid body and geometric restraints were used for the alkyl chains and THF ligands (U_{iso} for Hs was fixed to 0.08 Å²).

In the case of complex **22**, XPRED^[27] clearly indicated an orthorhombic *C* lattice type, but the examination of systematic absence exceptions showed only the presence of a 2₁ axis, while the mean $|E^2 - 1|$ was 1.102. Therefore, the suggested space group was accepted ($C222_1$). In the final stages of refinement, some rigid body and geometric restraints were applied to some alkyl chains. For one atom (C54), we were able to determine two spatial positions, A and B, (occupancy factor for site A = 0.61(2)) and include them into the model (U_{iso} for Hs was fixed to 0.08 Å²).

Extreme disorder affected the naphthalene ring in complex **23**, because the arene can adopt two dispositions which maintain the six-membered ring linked to barium in the same place (occupancy factor for disposition A = 0.52(1)). Geometric constraints and restraints were applied by using AFIX 116 and DFIX instructions in order to find reasonable parameters. Some other geometric restraints were applied to alkyl chains and hydrogens were not included into the model. Structure refinement, molecular graphics, and geometric calculations were carried out on all structures with the SHELXTL software package, release 5.1.^[28] Crystallographic data (excluding structure factors) for the structures reported in this paper have been deposited with the Cambridge Crystallographic Data Centre as supplementary publication no. CCDC-150075 (**7**), CCDC-150076 (**10**), CCDC-152180 (**13a**), CCDC-152181 (**13b**), CCDC-112148 (**14**), CCDC-150077 (**15**), CCDC-150078 (**18**), CCDC-112149 (**19**), CCDC-150079 (**22**), CCDC-150080 (**23**), CCDC-152182 (**24**), and CCDC-152183 (**25**). Copies of the data can be obtained free of charge on application to CCDC, 12 Union Road, Cambridge CB2 1EZ, UK (fax: (+44) 1223-336-033; e-mail: deposit@ccdc.cam.ac.uk).

Acknowledgements

We thank the “Fonds National Suisse de la Recherche Scientifique” (Bern, Switzerland, Grant No. 20-53336.98), Action COST D9 (European Program for Scientific Research, OFES No. C98.008), and Fondation Herbette (University of Lausanne, N. Re) for financial support.

- [1] a) J. C. Ma, D. A. Dougherty, *Chem. Rev.* **1997**, *97*, 1303–1324; b) D. A. Dougherty, *Science* **1996**, *271*, 163–168; c) J. Sunner, K. Nishizawa, P. Kebarle, *J. Phys. Chem.* **1981**, *85*, 1814–1820.
- [2] a) S. K. Burley, G. A. Petsko, *FEBS Lett.* **1986**, *203*, 139–143; b) N. S. Scrutton, A. R. C. Raine, *Biochem. J.* **1996**, *319*, 1–8.
- [3] a) T. J. Sheppard, M. A. Petti, D. A. Dougherty, *J. Am. Chem. Soc.* **1986**, *108*, 6085–6087; b) T. J. Sheppard, M. A. Petti, D. A. Dougherty, *J. Am. Chem. Soc.* **1986**, *108*, 1983–1985; c) M. A. Petti, T. J. Sheppard, J. R. E. Barrans, D. A. Dougherty, *J. Am. Chem. Soc.* **1988**, *110*, 6825–6840.
- [4] a) G. W. Rabe, L. M. Liable-Sands, C. D. Incarvito, K.-C. Lam, A. L. Rheingold, *Inorg. Chem.* **1999**, *38*, 4342–4346; b) G. W. Rabe, S.

Table 3. Crystal data and details of the structure determination for **7**, **10**, **14**, **15**, **18**, **19**, **22**, and **23**.

	7	10	14	15
formula	C ₄₈ H ₇₆ CS ₄ N ₄ O ₆	C ₆₆ H ₁₁₀ K ₄ N ₄ O ₆ · C ₄ H ₈ O	C ₅₂ H ₈₀ Ca ₂ N ₄ O ₄ · C ₄ H ₈ O	C ₅₂ H ₈₀ N ₄ O ₄ Sr ₂
M _r	1336.77	1187.96	977.46	1072.54
crystal system	orthorhombic	monoclinic	tetragonal	tetragonal
space group	<i>Pmma</i>	<i>I2/a</i>	<i>I4₁/a</i>	<i>I4₁/a</i>
a [Å]	20.7748(17)	21.356(3)	14.4379(14)	14.460(2)
b [Å]	12.0341(10)	29.534(3)	14.4379(14)	14.460(2)
c [Å]	10.3486(5)	23.358(3)	30.636(3)	31.416(9)
β [°]	90	110.531(14)	90	90
V [Å ³]	2587.2(3)	13797(3)	6386.2(11)	6569(2)
Z	2	8	4	4
ρ _{calcd} [g cm ⁻³]	1.716	1.144	1.017	1.085
F(000)	1320	5168	2128	2272
μ [mm ⁻¹]	2.844	0.306	0.220	1.665
T [K]	143	143	143	143
λ [Å]	0.71073	0.71073	0.71073	0.71070
measured reflections	13 665	38 525	17 816	19 753
observed reflections	2422	11 557	2618	2720
unique reflections [I > 2σ(I)]	2306	9678	2283	2137
parameters	149	754	186	186
R ^[a] [I > 2σ(I)]	0.0811	0.0771	0.0643	0.0581
wR2 ^[a] (all data)	0.2218	0.1876	0.2125	0.2200
GoF ^[b]	1.080	1.104	1.167	1.176
	18	19	22	23
formula	C ₆₈ H ₁₁₂ Ba ₂ N ₄ O ₄	C ₄₈ H ₇₂ CaLi ₂ N ₄ O ₃	C ₇₂ H ₁₀₈ Ba ₂ N ₄	C ₇₂ H ₉₆ Ba ₂ N ₄
M _r	1324.30	807.06	1304.30	1292.21
crystal system	orthorhombic	monoclinic	orthorhombic	monoclinic
space group	<i>Fddd</i>	<i>P2/n</i>	<i>C22₁</i>	<i>C2/c</i>
a [Å]	15.779(3)	16.4093(13)	27.923(3)	27.690(6)
b [Å]	28.804(6)	15.0183(12)	31.274(3)	18.898(4)
c [Å]	29.721(6)	18.9238(13)	15.684(3)	19.579(4)
β [°]	90	90.728(6)	90	134.99(3)
V [Å ³]	13508(5)	4663.2(6)	13696(3)	7246(3)
Z	8	4	8	4
ρ _{calcd} [g cm ⁻³]	1.302	1.150	1.265	1.185
F(000)	5536	1752	5440	2672
μ [mm ⁻¹]	1.206	0.177	1.184	1.119
T [K]	143	143	143	143
λ [Å]	0.71070	0.71073	0.71070	0.71070
measured reflections	15 214	33 828	26 572	18 962
observed reflections	2684	10 621	10 210	58 19
unique reflections [I > 2σ(I)]	1873	7828	9306	4583
parameters	179	526	717	217
R ^[a] [I > 2σ(I)]	0.0847	0.0656	0.0660	0.0881
wR2 ^[a] (all data)	0.2656	0.1761	0.1967	0.2681
GoF ^[b]	1.060	1.066	1.095	1.055

[a] $R = \frac{\sum |F_o| - |F_c|}{\sum |F_o|}$, $wR2 = \frac{\{\sum [w(F_o^2 - F_c^2)^2] / \sum [w(F_o^2)^2]\}^{1/2}}$; [b] $GoF = \frac{\{\sum [w(F_o^2 - F_c^2)^2] / (n - p)\}^{1/2}}$, in which n is the number of data and p is the number of parameters refined.

- Kheradmandan, L. M. Liabé-Sands, I. A. Guzei, A. L. Rheingold, *Angew. Chem.* **1998**, *110*, 1495–1497; *Angew. Chem. Int. Ed.* **1998**, *37*, 1404–1407.
- [5] S. L. De Wall, E. S. Meadows, L. J. Barbour, G. W. Gokel, *J. Am. Chem. Soc.* **1999**, *121*, 5613–5614.
- [6] M. O. Senge, *Angew. Chem.* **1996**, *108*, 2051–2053; *Angew. Chem. Int. Ed. Engl.* **1996**, *35*, 1923–1925, and references therein.
- [7] E. Weiss, *Angew. Chem.* **1993**, *105*, 1565–1587; *Angew. Chem. Int. Ed. Engl.* **1993**, *32*, 1501–1523.
- [8] a) D. Jacoby, E. Solari, C. Floriani, A. Chiesi-Villa, C. Rizzoli, *J. Am. Chem. Soc.* **1993**, *115*, 3595–3602; b) D. Jacoby, S. Isoz, E. Solari, C. Floriani, A. Chiesi-Villa, C. Rizzoli, *J. Am. Chem. Soc.* **1995**, *117*, 2793–2804; c) S. De Angelis, E. Solari, C. Floriani, A. Chiesi-Villa, C. Rizzoli, *Angew. Chem.* **1995**, *107*, 1200–1202; *Angew. Chem. Int. Ed. Engl.* **1995**, *34*, 1092–1094; d) D. Jacoby, S. Isoz, E. Solari, C. Floriani, K. Schenk, A. Chiesi-Villa, C. Rizzoli, *Organometallics* **1995**, *14*, 4816–4824; e) G. Solari, E. Solari, C. Floriani, A. Chiesi-Villa, C. Rizzoli, *Organometallics* **1997**, *16*, 508–510; f) D. Jacoby, S. Isoz, E. Solari, C. Floriani, A. Chiesi-Villa, C. Rizzoli, *J. Am. Chem. Soc.* **1995**, *117*, 2805–2816.
- [9] D. E. Fenton, in *Comprehensive Coordination Chemistry* (Eds.: G. Wilkinson, R. D. Gillard, J. A. McCleverty), Pergamon, Oxford, **1987**, Chapter 33.
- [10] Review on the chemistry of hetero-s-block metals: R. E. Mulvey, *Chem. Soc. Rev.* **1998**, *27*, 339–346.
- [11] a) F. Inokuchi, Y. Miyahara, T. Inazu, S. Shinkai, *Angew. Chem.* **1995**, *107*, 1459–1462; *Angew. Chem. Int. Ed. Engl.* **1995**, *34*, 1364–1366; b) A. Zanotti-Gerosa, E. Solari, L. Giannini, C. Floriani, A. Chiesi-Villa, C. Rizzoli, *Chem. Commun.* **1997**, 183–184, and references therein.
- [12] L. Bonomo, O. Dandin, E. Solari, C. Floriani, R. Scopelliti, *Angew. Chem.* **1999**, *111*, 963–966; *Angew. Chem. Int. Ed.* **1999**, *38*, 913–915.

- [13] C. Floriani, *Pure Appl. Chem.* **1996**, *68*, 1–8, and references therein.
- [14] C. Floriani, R. Floriani-Moro, in *The Porphyrin Handbook, Vol. 3* (Eds.: K. M. Kadish, K. M. Smith, R. Guilard), Academic Press, Burlington, MA, **1999**, Chapters 24 and 25, and references therein.
- [15] For alkali metal porphyrins, see: J. Arnold, *The Porphyrin Handbook, Vol. 3* (Eds.: K. M. Kadish, K. M. Smith, R. Guilard), Academic Press, Burlington, MA, **1999**, Chapter 17, and references therein.
- [16] a) M. A. Beswick, D. S. Wright, in *Comprehensive Organometallic Chemistry II, Vol. 1* (Eds.: E. W. Abel, F. G. A. Stone, G. Wilkinson, C. E. Housecroft), Pergamon, Oxford, **1995**, Chapter 1; b) T. A. Hanusa, *Chem Rev.* **1993**, *93*, 1023–1036.
- [17] G. Rabe, H. W. Roesky, D. Stalke, F. Pauer, G. M. Sheldrick, *J. Organomet. Chem.* **1991**, *403*, 11–19.
- [18] L. Bonomo, E. Solari, C. Floriani, unpublished results.
- [19] Active calcium was prepared according to a known procedure: T. C. Wu, H. Xiong, R. D. Rieke, *J. Org. Chem.* **1990**, *55*, 5045–5051.
- [20] M. J. Harvey, T. P. Hanusa, V. G. Young, Jr., *Angew. Chem.* **1999**, *111*, 241–242. *Angew. Chem. Int. Ed.* **1999**, *38*, 217–219.
- [21] A. F. Wells, *Structural Inorganic Chemistry, 5th Edition*, Oxford University, Oxford (UK), **1984**, p. 1285.
- [22] a) *Comprehensive Organometallic Chemistry II, Vol. 1* (Eds.: E. W. Abel, F. G. A. Stone, G. Wilkinson, C. E. Housecroft), Pergamon, Oxford, **1995**, p. 113; b) R. A. Williams, T. P. Hanusa, J. C. Huffman, *Organometallics* **1990**, *9*, 1128–1134; c) C. J. Burns, R. A. Andersen, *J. Organomet. Chem.* **1987**, *325*, 31; d) M. J. McCormick, R. A. Williams, L. J. Levine, T. P. Hanusa, *Polyhedron* **1988**, *7*, 725; e) T. P. Hanusa, *Polyhedron* **1990**, *9*, 1345; f) R. A. Williams, K. F. Tesh, T. P. Hanusa, *J. Am. Chem. Soc.* **1991**, *113*, 4383; g) R. A. Williams, T. P. Hanusa, J. C. Huffman, *J. Organomet. Chem.* **1992**, *429*, 143; h) D. J. Burkey, R. A. Williams, T. P. Hanusa, *Organometallics* **1993**, *12*, 1331; i) P. S. Tanner, T. P. Hanusa, *Polyhedron* **1994**, *13*, 2417; j) M. Westerhausen, M. Hartmann, W. Schwarz, *J. Organomet. Chem.* **1995**, *501*, 359; k) J. S. Overby, T. P. Hanusa, *Organometallics* **1996**, *15*, 2205.
- [23] M. Westerhausen, M. Krafta, N. Wiberg, H. Noth, A. Pfitzner, *Z. Naturforsch. Teil B* **1998**, *53*, 1489.
- [24] Z. Otwinowski, W. Minor, *Methods in Enzymology, Vol. 276, Part A* (Eds.: C. W. Carter, Jr., R. M. Sweet), Academic, New York, **1997**, 307–326.
- [25] Kuma Diffraction Instruments GmbH, PSE-EPFL module 3.4, CH-1015, Lausanne, Switzerland, **2000**.
- [26] A. Altomare, M. C. Burla, M. Camalli, G. L. Casciarano, C. Giacovazzo, A. Guagliardi, A. G. G. Moliterni, G. Polidori, R. Spagna, *J. Appl. Crystallogr.* **1999**, *32*, 115–119.
- [27] *Data Preparation and Reciprocal Space Exploration*, Bruker AXS, Madison, Wisconsin, 53719 (USA), **1997**.
- [28] Bruker AXS, Madison, Wisconsin, 53719, (USA), **1997**.

Received: September 14, 2000 [F2729]